



INCREASED PINNING IN “ $\text{Bi}_2\text{Sr}_2\text{CaCu}_2\text{O}_8$ ” CERAMICS

PETER MAJEWSKI¹, BERNHARD HETTICH², STEFFEN ELSCHNER² and FRITZ ALDINGER¹

¹Max-Planck-Institut für Metallforschung, Institut für Werkstoffwissenschaft, Heisenbergstr. 5, 70569 Stuttgart and ²Hoechst AG, Corporate Research, D-65926 Frankfurt am Main, Germany

(Received 3 September 1993)

Abstract—From a consideration of the phase equilibrium diagram of the system Bi_2O_3 – SrO – CaO – CuO , a simple annealing procedure was developed to transform single phase 2212 ceramics with compositions $\text{Bi}_{2.18}\text{Sr}_{1.75}\text{Ca}_{1.25}\text{Cu}_2\text{O}_{8+d}$ and $\text{Bi}_{2.3}\text{Sr}_2\text{CaCu}_2\text{O}_{8+d}$ into multi phase samples containing Ca_2CuO_3 and/or liquid. The transformations result in increases of the critical current densities at 1 T of 5–10 times, which is believed to reflect the increased pinning properties of these ceramics. The exact nature of the resulting pinning centres has not been determined yet.

INTRODUCTION

“ $\text{Bi}_2\text{Sr}_2\text{CaCu}_2\text{O}_8$ ” (2212 phase, $T_c \leq 94$ K) exhibits weak internal pinning at temperatures above 20–30 K resulting in a decrease of the critical current density of more than two orders of magnitude in an applied magnetic field of about 1 T [1–3]. Therefore, an application of the 2212 phase material in devices under magnetic fields has not been possible. Based on the observation of Murakami *et al.* [4], who increased the pinning of Y–Ba–Cu–O ceramics by the introduction of the second phase Y_2BaCuO_5 , several investigations [5, 6] have claimed Ca_2CuO_3 increases the pinning of 2212 and the 2223 phase ($[\text{Bi,Pb}]_2\text{Sr}_2\text{Ca}_2\text{Cu}_3\text{O}_{10}$) ceramics. However, the grains of powder metallurgically prepared ceramics are much too large (1–100 μm) to act as effective pinning centres which are assumed to be smaller than 10 nm [7, 8]. The aim of this work is to reveal a processing route resulting in Bi-type superconducting bulk ceramics with very fine ($\leq 1 \mu\text{m}$) precipitates of second phases and enhanced pinning properties using temperature dependent solubility lines.

EXPERIMENTAL

Two samples have been prepared, the compositions of which are $\text{Bi}_{2.18}\text{Sr}_{1.75}\text{Ca}_{1.25}\text{Cu}_2\text{O}_{8+d}$ (batch 1) and $\text{Bi}_{2.3}\text{Sr}_2\text{CaCu}_2\text{O}_{8+d}$ (batch 2), using Bi_2O_3 , SrCO_3 , CaCO_3 and CuO starting materials (purity 99%). The mixed and ground powders were calcined at 750 and 800°C for 24 h and pressed into cylindric pellets (15 mm long and 4 mm in diameter, 625 MPa). The pellets were sintered at 820°C in air for 48 h in the single phase region, furnace cooled and subsequently annealed at 885°C for 10, 15, 22.5, 25, 30, 37.5, 45 and 60 min (batch 1) and 15, 30, 45 and 60 (batch 2) min in air in the heterogeneous phase regions and finally quenched on a cold copper plate in air (Figs 1 and 2). The critical current densities of the pellets have been obtained by measuring the magnetic susceptibility at 30 K up to 1 T and calculating J_c from these data using Bean’s model [11]. The magnetic susceptibility has been measured at 30 K, as at this temperature an increase of the pinning properties is expected to become most pronounced. The porosity and the second phase content of the samples have been determined by optical and electron microscopy. The critical temperatures (onset) of the pellets have been determined by a.c. susceptibility measurements. Phase identification has been performed using electron microscopy with energy dispersive X-ray analysis (EDX) and optical microscopy using polarized light.

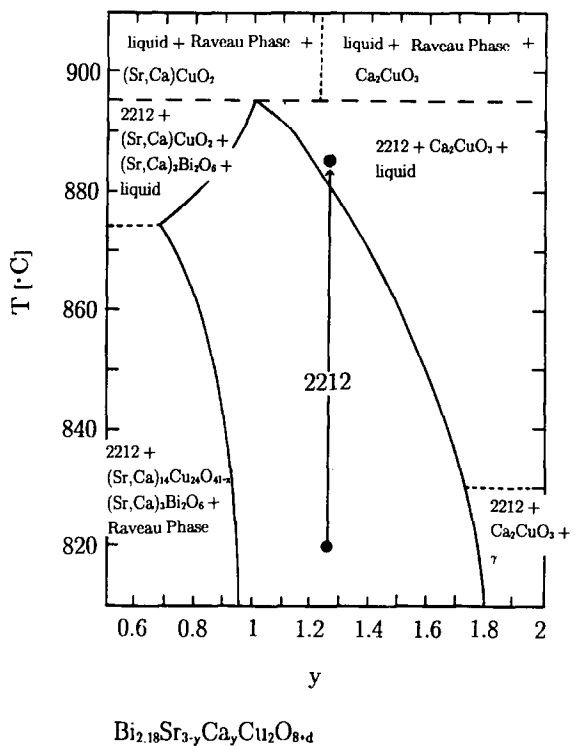


Fig. 1. Section of the phase diagram showing the melting temperature vs Ca content [9, 10] including a line indicating the annealing step to precipitate Ca_2CuO_3 + liquid.

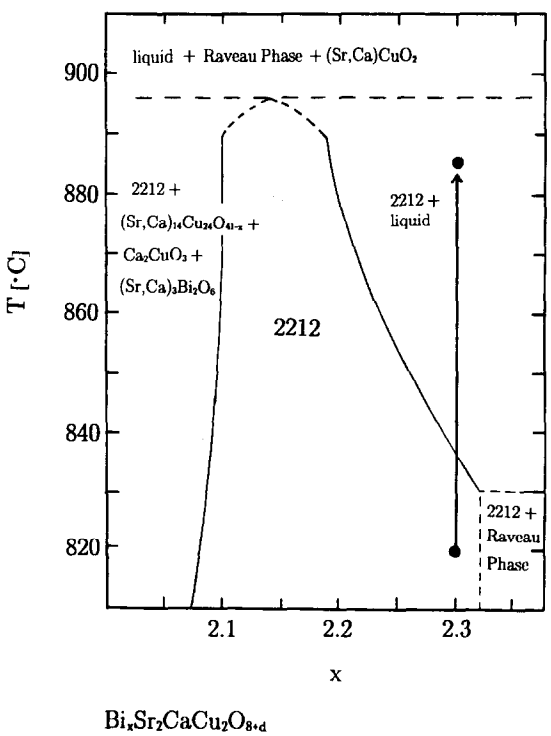


Fig. 2. Section of the phase diagram showing the melting temperature vs Bi content [9, 10] including a line indicating the annealing step to precipitate liquid.

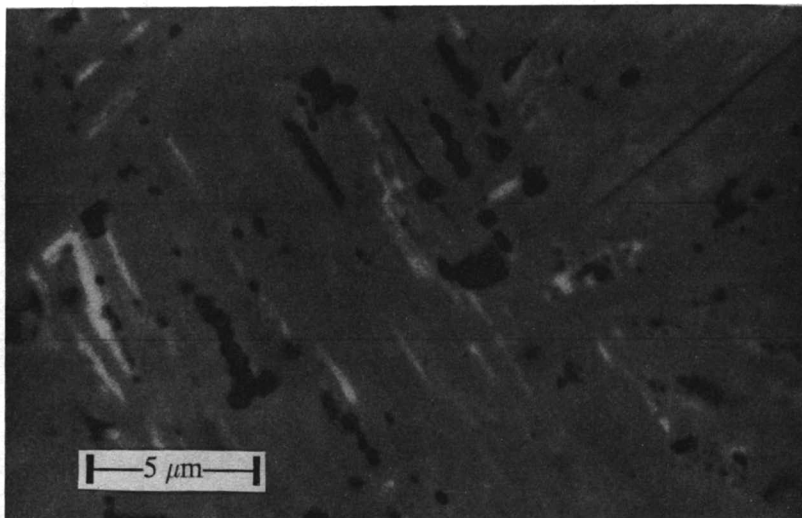


Fig. 3. SEM/BSE image of 2212 phase (grey) of a post annealed sample of batch 1 containing Ca_2CuO_3 (black) crystals and a liquid phase (white).

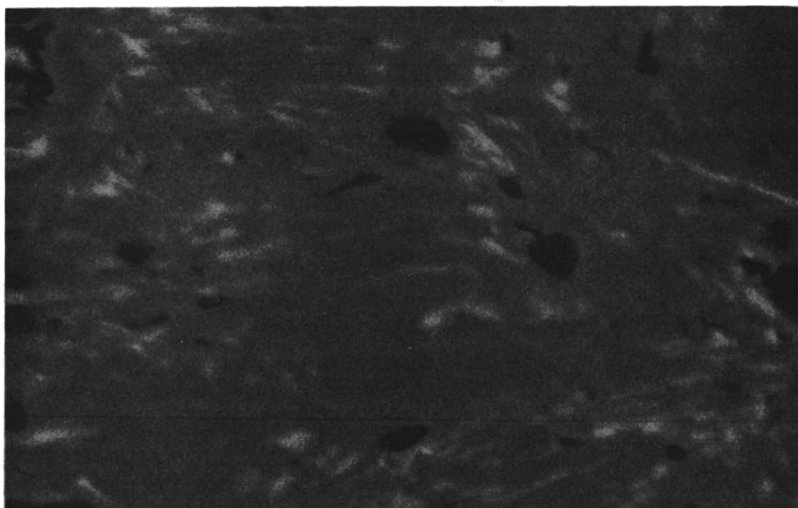


Fig. 4. SEM/BSE image of 2212 phase (grey) of a post annealed sample of batch 2 containing a liquid phase (white). Black spots: pores.

RESULTS

The sintered starting “2212” samples are single phase (>99 vol.%) by X-ray analysis, as well as, by electron and optical microscopy. According to the phase equilibria, the annealing of the samples of batch 1 results in the formation of Ca_2CuO_3 and liquid (Fig. 3), whereas, annealing the samples of batch 2 results only in a liquid phase in addition to the 2212 phase and no cuprate (Fig. 4). With the formation of these second phases the chemical composition of the 2212 phase changes. The Ca content of the 2212 phase of batch 1 decreases from 17.1 to 16.1 mol.%. The Bi content of the 2212 phase of batch 2 decreases from 31.5 to 29.6 mol.%. The mean grain size of the Ca_2CuO_3 crystals is about 100 nm after an annealing of 15 min and increases with the annealing time to about 200–300 nm after 30 min (Fig. 3) and about 500 nm after 45 min. The liquid forms in both samples in regularly shaped streaks, which also grow with increasing annealing time.

Figure 5 shows the susceptibility vs temperature plots of a starting sample and the 30 min post

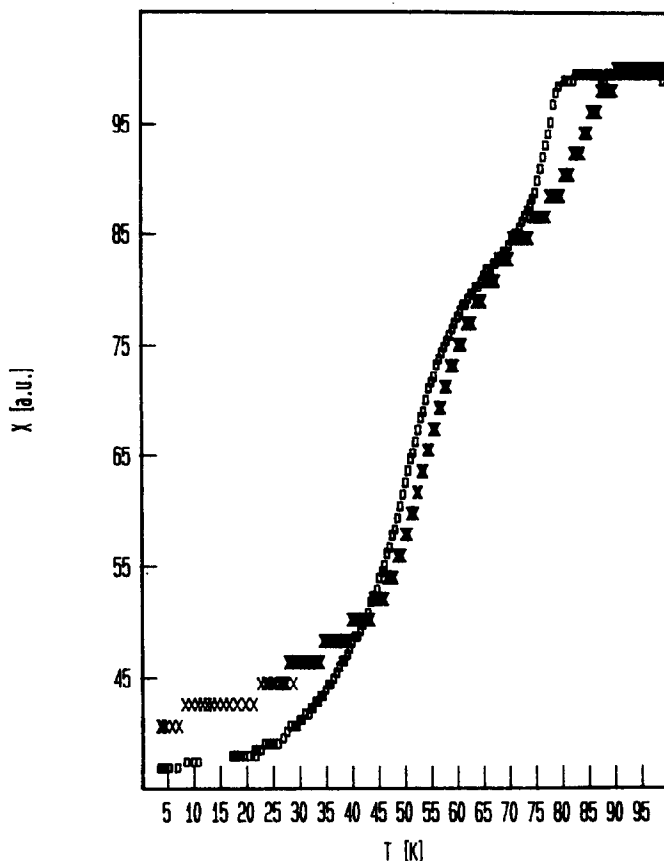
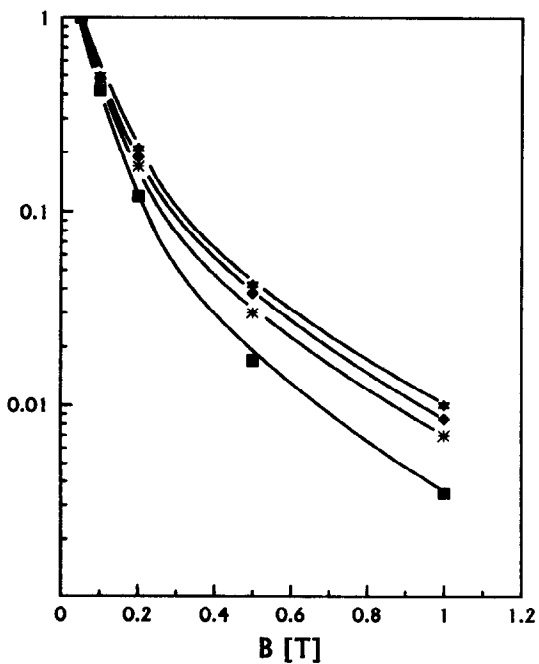


Fig. 5. Susceptibility vs temperature plot of the starting sample (squares) and the 30 min annealed sample (crosses) of batch 1.

$J_c(B)/J_c(0.05 \text{ T})$



$J_c(B)/J_c(0.05 \text{ T})$

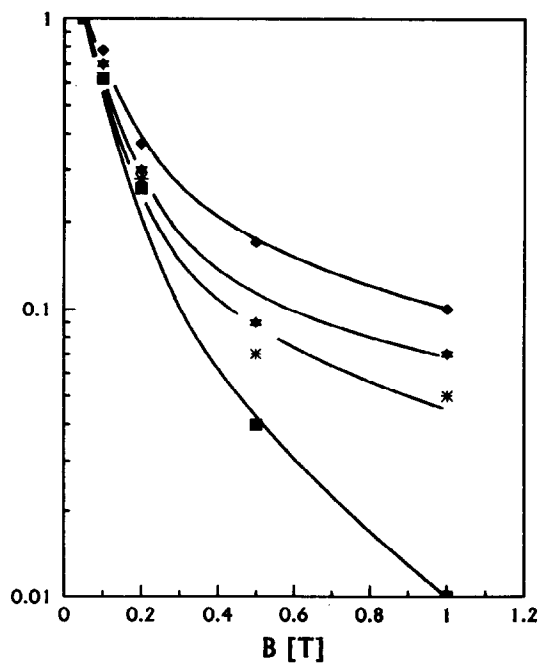


Fig. 6. $J_{c(B)}/J_{c(0.05 \text{ T})}$ at 30 K vs the applied magnetic field B for different annealing times; (a) Batch 1; (b) batch 2. Squares: starting sample; stars: 15 min; rhombs: 30 min; crosses: 45 min.

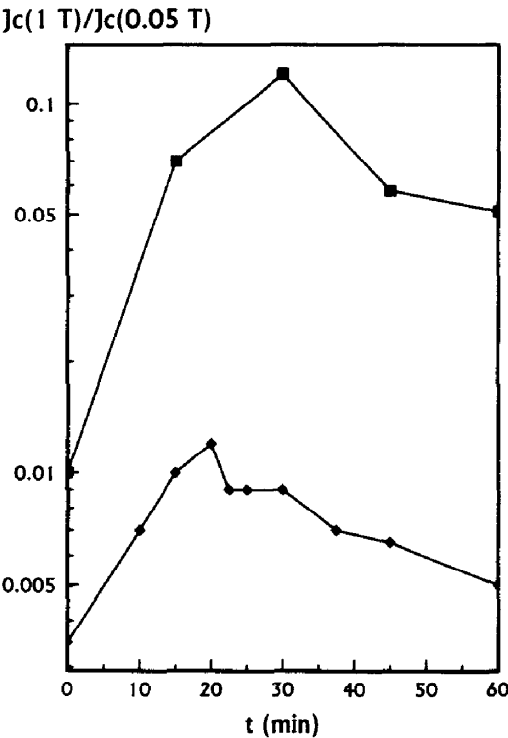


Fig. 7. $J_{c(1\text{ T})}/J_{c(0.05\text{ T})}$ at 30 K vs the post annealing time of the samples of batch 1 (rhombs) and batch 2 (squares).

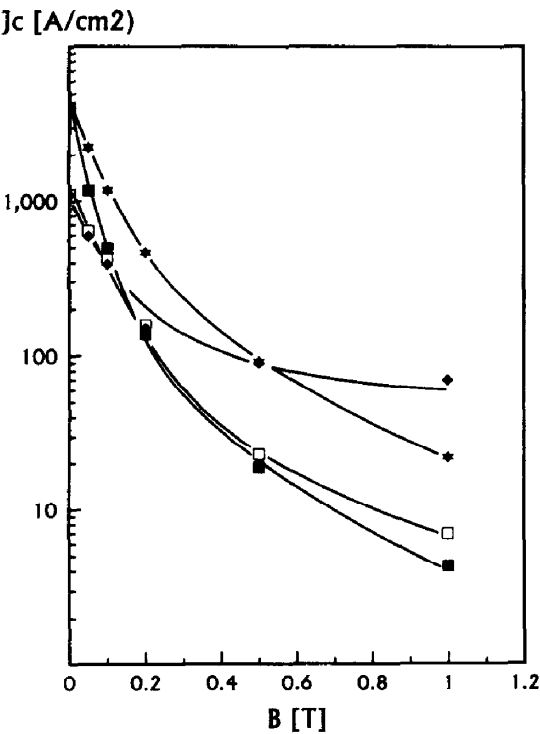


Fig. 8. J_c vs the applied magnetic field of the starting sample (squares: batch 1; solid squares: batch 2) and the 15 min annealed sample (stars) of batch 1 and the 30 min annealed sample (rhombs) of batch 2.

annealed sample of batch 1. It is seen that the critical temperature T_c of the sample and the trend of the susceptibility line have not been changed significantly by the post annealing ($\Delta T_c \simeq 5$ K).

In Fig. 6(a, b) the ratio of the J_c at the applied magnetic field B to the J_c at 0.05 T of the samples ($J_{c(B)}/J_{c(0.05\text{ T})}$), which represent the pinning force, is plotted vs the applied magnetic field B in order to rule out a possible influence of the sample shape, cracks etc. The diagrams show, that the post annealed samples exhibit a less pronounced decrease of J_c with increasing magnetic field up to 1 T compared to the starting samples, which indicates increased pinning properties of the post annealed samples.

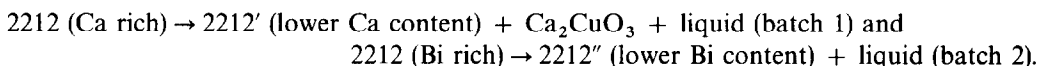
The graphic analysis (Fig.7) clearly shows that the $J_{c(1\text{ T})}/J_{c(0.05\text{ T})}$ values exhibit a distinct maximum at an annealing time of about 20 min for batch 1 and at 30 min for batch 2. With increasing and decreasing annealing time the values decrease.

The J_c vs B plot of the starting samples and the 15 min annealed sample of batch 1 and the 30 min annealed sample of batch 2 are depicted in Fig. 8. The samples of batch 1 and 2 have a J_c of 4000 and 1100 A/cm² at zero magnetic field, respectively. At 0.2 T the J_c of the annealed sample of batch 1 is about 1.5 times larger compared to the J_c of the starting sample. With increasing magnetic field the difference between the J_c of the annealed sample and the starting sample increases. At 1 T the J_c of the annealed samples is about five times larger compared to the J_c of the starting sample. Considering the samples of batch 2 the difference between the J_c of the annealed sample and the starting sample increases from a factor of 1 at 0.2 T to a factor of 10 at 1 T.

DISCUSSION

The observed increase of the J_c at magnetic fields above 0.2 T of the post annealed samples shows strong evidence for increased pinning properties of these samples. The fact that the annealed samples of batch 2 exhibit increased pinning indicates that the quenched liquid phase particles might cause this effect and that Ca_2CuO_3 does not exclusively cause the increased pinning, if at all. The decrease of the pinning effect with increasing annealing time might be due to coarsening of the second phases.

However, it has to be taken into account that besides the effect of such second phases the increased pinning can also be caused by defects in the 2212 phase itself resulting from the phase transformation due to the reactions:



Such defects could be e.g. lattice distortions which may act as pinning centres. In this case, the observed decrease of J_c with increasing annealing time could be explained by the defect healing.

However, none of the potential pinning centres have been directly verified and further detailed investigations have to be performed to clarify the nature of the pinning centres. Nevertheless, the experiments show that it is possible in principle to introduce artificial pinning in bulk ceramics of the 2212 phase, although the absolute J_c values of the ceramic samples are quite low.

CONCLUSION

Single 2212 phase ceramics with the composition $\text{Bi}_{2.18}\text{Sr}_{1.75}\text{Ca}_{1.25}\text{Cu}_2\text{O}_{8+d}$ and $\text{Bi}_{2.3}\text{Sr}_2\text{CaCu}_2\text{O}_{8+d}$ have been heat treated by a simple annealing step to transform them into multi phase samples. The transformations result in increases of the critical current densities of five to ten times under an external magnetic field of 1 T, which is due to the generation of effective pinning centres in the 2212 phase ceramics by this process. Further investigations to clarify the nature of the produced pinning centres are in progress.

REFERENCES

1. H. Krauth, K. Heine and J. Tenbrink, *High-Temperature Superconductors—Materials Aspects* (Edited by H.C. Freyhardt, R. Flükiger and M. Peuckert), p. 29. DGM, Oberursel, F.R.G. (1991).
2. K. Togano, H. Kumakura, H. Maeda and J. Kase, *Chemistry of High Temperature Superconductors* (Edited by C.N.R. Rao), p. 399. World Scientific, London (1991).

3. J. Bock, S. Elschner and E. Preisler, *Advances in Superconductivity III* (Edited by K. Kajimura and H. Hayakawa), p. 797. Proc. ISS 1990, Sendai. Springer, Berlin (1991).
4. M. Murakami, H. Fujimoto, T. Oyama, S. Gotho, Y. Shiohara, N. Koshizuka and S. Tanaka, *High-Temperature Superconductors—Materials Aspects* (Edited by H.C. Freyhardt, R. Flükiger and M. Peuckert), p. 13. DGM, Oberursel, F.R.G. (1991).
5. D. Shi, M. S. Boley, U. Welp, J. G. Chen and Y. Liao, *Phys. Rev. B* **40**, 5255 (1989).
6. T. Umemura, K. Egawa, S. Kinouchi, M. Wakata and S. Utsunomiya, *Physica C* **185–189** 2219 (1991).
7. J. Boiko, P. Majewski and F. Aldinger, *Z. f. Metallke* (1994). In press.
8. E. H. Brandt, *Physica C* **195**, 1 (1992).
9. P. Majewski and B. Hettich, *MRS Proc.* **275**, 627 (1992).
10. P. Majewski, B. Hettich, N. Rüffer and F. Aldinger, *J. Elect. Mat.* (1994). In press.
11. C. P. Bean, *Phys. Rev. Lett.* **8**, 250 (1962).